

Earth's ion upflow associated with polar cap patches: global and in-situ observations

Article

Published Version

Zhang, Q.-H., Zong, Q.-G., Lockwood, M., Heelis, R. A., Hairston, M., Liang, J., McCrea, I., Zhang, B.-C., Moen, J., Zhang, S.-R., Zhang, Y.-L., Ruohoniemi, J. M., Lester, M., Thomas, E. G., Liu, R.-Y., Dunlop, M. W., Liu, Y. C.-M. and Ma, Y.-Z. (2016) Earth's ion upflow associated with polar cap patches: global and in-situ observations. *Geophysical Research Letters*, 43 (5). pp. 1845-1853. ISSN 0094-8276 doi: <https://doi.org/10.1002/2016GL067897> Available at <http://centaur.reading.ac.uk/58514/>

It is advisable to refer to the publisher's version if you intend to cite from the work.

Published version at: <http://dx.doi.org/10.1002/2016GL067897>

To link to this article DOI: <http://dx.doi.org/10.1002/2016GL067897>

Publisher: American Geophysical Union

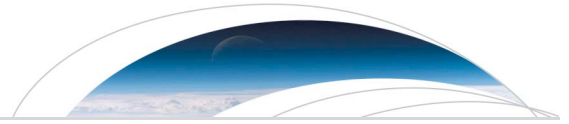
All outputs in CentAUR are protected by Intellectual Property Rights law, including copyright law. Copyright and IPR is retained by the creators or other copyright holders. Terms and conditions for use of this material are defined in the [End User Agreement](#).

www.reading.ac.uk/centaur

CentAUR

Central Archive at the University of Reading

Reading's research outputs online



RESEARCH LETTER

10.1002/2016GL067897

Key Points:

- First simultaneous global monitoring of patch and in situ observation of ion upflow in the polar cap
- Strong fluxes of upwelling O^+ originating from frictional heating produced by rapid flow of patch
- Rapidly moving patches can provide an important source of upwelling ions

Supporting Information:

- Figure S1

Correspondence to:

Q.-H. Zhang,
zhangqinghe@sdu.edu.cn

Citation:

Zhang, Q.-H., et al. (2016), Earth's ion upflow associated with polar cap patches: Global and in situ observations, *Geophys. Res. Lett.*, 43, 1845–1853, doi:10.1002/2016GL067897.

Received 21 JAN 2016

Accepted 19 FEB 2016

Accepted article online 22 FEB 2016

Published online 8 MAR 2016

Earth's ion upflow associated with polar cap patches: Global and in situ observations

Qing-He Zhang¹, Qiu-Gang Zong², Michael Lockwood³, Roderick A. Heelis⁴, Marc Hairston⁴, Jun Liang⁵, Ian McCrea⁶, Bei-Chen Zhang⁷, Jøran Moen⁸, Shun-Rong Zhang⁹, Yong-Liang Zhang¹⁰, J. Michael Ruohoniemi¹¹, Mark Lester¹², Evan G. Thomas¹¹, Rui-Yuan Liu⁷, Malcolm W. Dunlop⁶, Yong C.-M. Liu¹³, and Yu-Zhang Ma¹

¹Shandong Provincial Key Laboratory of Optical Astronomy and Solar-Terrestrial Environment, Institute of Space Sciences, Shandong University, Weihai, China, ²School of Earth and Space Sciences, Peking University, Beijing, China, ³Department of Meteorology, University of Reading, Reading, UK, ⁴William B. Hanson Center for Space Sciences, University of Texas at Dallas, Richardson, Texas, USA, ⁵Department of Physics and Astronomy, University of Calgary, Calgary, Alberta, Canada, ⁶Space Sciences Division, Rutherford Appleton Laboratory, Didcot, UK, ⁷SOA Key Laboratory for Polar Science, Polar Research Institute of China, Shanghai, China, ⁸Department of Physics, University of Oslo, Oslo, Norway, ⁹MIT Haystack Observatory, Westford, Massachusetts, USA, ¹⁰The Johns Hopkins University Applied Physics Laboratory, Laurel, Maryland, USA, ¹¹Bradley Department of Electrical and Computer Engineering, Virginia Polytechnic Institute and State University, Blacksburg, Virginia, USA, ¹²Department of Physics and Astronomy, University of Leicester, Leicester, UK, ¹³State Key Laboratory of Space Weather, Center for Space Science and Applied Research, Chinese Academy of Sciences, Beijing, China

Abstract We report simultaneous global monitoring of a patch of ionization and in situ observation of ion upflow at the center of the polar cap region during a geomagnetic storm. Our observations indicate strong fluxes of upwelling O^+ ions originating from frictional heating produced by rapid antisunward flow of the plasma patch. The statistical results from the crossings of the central polar cap region by Defense Meteorological Satellite Program F16–F18 from 2010 to 2013 confirm that the field-aligned flow can turn upward when rapid antisunward flows appear, with consequent significant frictional heating of the ions, which overcomes the gravity effect. We suggest that such rapidly moving patches can provide an important source of upwelling ions in a region where downward flows are usually expected. These observations give new insight into the processes of ionosphere-magnetosphere coupling.

1. Introduction

Ion outflow from the Earth's ionosphere is an important aspect of magnetosphere-ionosphere-thermosphere coupling, as it provides a significant, and at times dominant, source of magnetospheric plasma [Shelley et al., 1972; Lockwood and Titheridge, 1981; Yau and Andre, 1997; Andre and Yau, 1997; Moore et al., 1997; Chappell et al., 2000]. Such outflow potentially has a global impact on the entire Sun-Earth system through its ability to affect plasma transport and convection in the magnetosphere. The presence of heavier ionospheric ions, such as O^+ , may also influence the onset of magnetic reconnection at both the dayside magnetopause and the nightside magnetotail and the triggering of magnetic storms and substorms [Moore et al., 1997; Daglis, 1997; Winglee, 2004; Yau et al., 2011]. Ion outflow may also modulate atmospheric isotope abundances on geological timescales, depending on the fraction of upflowing ions that subsequently returns to the ionosphere and the fraction that is ejected into interplanetary space [Axford, 1968; Seki et al., 2001]. Ion outflows from the auroral and polar cap ionosphere fall into two categories, based on their flow speed. Bulk ion flows, including the polar wind and auroral bulk ion upflow (Figure S1 in the supporting information), exhibit thermal ion upflows with velocity <1500 m/s, whereas suprathermal ion outflows, including ion beams, ion conics, and upwelling ions, correspond to upward motion in excess of the escape velocity (>10 km/s) [Yau and Andre, 1997; Andre and Yau, 1997; Sharp et al., 1977; Yau et al., 2011; Semeter et al., 2003]. Thermal ion upflow in the topside ionosphere can supply ions to suprathermal ion outflows generated by various ion energization processes at higher altitudes [Yau and Andre, 1997; Andre and Yau, 1997; Moore et al., 1997; Strangeway et al., 2005; Sharp et al., 1977]. In other words, ion upflow occurs mainly at low altitude with thermal velocities and serve as the source for ion outflow at high altitudes where the ions achieve escape velocities.

Upflowing ions are thought to be energized from two different sources: (a) the flow of electromagnetic energy (Poynting flux), associated with the large-scale convection electric field, and (b) the deposition of particle

energy, primarily through soft electron precipitation [Strangeway et al., 2005; Skjæveland et al., 2011]. The enhanced Poynting flux leads to ion heating through Joule dissipation and/or various current-driven waves and instabilities in the lower ionosphere, leading to ion upwelling due to modification of the pressure gradient, while electron precipitation modifies the electron temperature and density in the *F* region ionosphere and in turn leads to an ambipolar electric field that accelerates ions upward [Strangeway et al., 2005; Ho et al., 1994]. Sometimes the electron and ion heating may accelerate the ions upward together in certain regions [Skjæveland et al., 2011, 2014].

It is generally accepted that much of the upward flow in the auroral zones and cusp is returned to the *F* region by downward flows in the polar cap [Redmon et al., 2010] (schematically shown in Figure S1). Indeed, an average picture of topside plasma flows shows the fluxes to be downward in the polar cap [Redmon et al., 2010; Stevenson et al., 2001]. However, it should be noted that rapid antisunward flows can produce significant ion frictional heating, leading to upward flows in the polar cap [Strangeway et al., 2005], where polar wind is often seen and simulated [Moore et al., 1997; Axford, 1968; Schunk and Sojka, 1989; Schunk, 2007], and a “tongue” of ionization and polar cap “patches” are often seen in the ionosphere [Foster et al., 2005; Crowley, 1996]. In the presence of enhanced plasma density, which may well accompany such enhanced plasma flows, significant upward fluxes of thermal plasma can result. This study provides direct evidence for this process, where the source plasma was found to be in a polar cap ionization patch and a high population of heavy ions occurred in the topside ionosphere. Such events, which exist on magnetic flux tubes that thread the magnetotail lobes [Yau and Andre, 1997; Andre and Yau, 1997; Moore et al., 1997; Strangeway et al., 2005; Sharp et al., 1977], may supply a plasma injection mechanism for escape to higher altitudes in the magnetosphere.

Polar cap patches are formed by ionospheric dynamics in the “cusp region” [Crowley, 1996; Carlson, 2012; Lockwood and Carlson, 1992; Valladares et al., 1999; Rodger et al., 1994; Zhang et al., 2011a]. They appear as islands of high-density plasma in a background that may be less than the patch density by 50% or more [Crowley, 1996; Carlson, 2012]. During periods of southward interplanetary magnetic field, they follow the flow streamlines of a two-cell convection pattern [Dungey, 1961; Zhang et al., 2013, 2015], moving across the pole from the dayside to the nightside, exiting the polar cap and entering the nightside auroral oval [Zhang et al., 2013, 2015; Oksavik et al., 2010; Hosokawa et al., 2009]. Simulations have shown that the locations of polar cap patches coincide with sites of enhanced upwelling H^+ produced by $O^+ + H \rightleftharpoons H^+ + O$ charge exchange in the propagating plasma patch [Schunk et al., 2005; Demars and Schunk, 2006; Gardner and Schunk, 2007]. However, it has been particularly difficult to study the correspondence between ion upflow and polar cap patches because of the limited data coverage of suitable instrumentation. Here we present a case study showing the dynamics of oxygen ion upflow associated with a polar cap patch. Our dataset combines ground-based global observations of the total electron content (TEC) provided by GPS receivers [Coster et al., 2003] and ionospheric plasma flows monitored by the Super Dual Auroral Radar Network (SuperDARN) radars [Greenwald et al., 1995; Chisham et al., 2007], along with in situ plasma and magnetic field measurements from the Defense Meteorological Satellite Program (DMSP) F16 and F17 satellites [Hardy et al., 1984].

2. Observations and Results

On 26 September 2011, a coronal mass ejection (CME) encountered Earth’s magnetopause at 12:37 UT, providing two enhancements of solar wind dynamic pressure, P_{dyn} , and producing a major geomagnetic storm [Zhang et al., 2013]. There was large and variable interplanetary magnetic field (IMF) at Earth with two intervals of exceptionally strong southward field (B_z , in red in Figure 1a) ahead of the second pressure pulse (Figure 1b). Southward IMF intervals favor rapid reconnection at the dayside magnetopause and are expected to generate pulsed ionospheric flows [Zhang et al., 2011b], which have frequently been implicated in patch production [Lockwood and Carlson, 1992; Zhang et al., 2011a]. Note that the IMF B_z decreased and B_y increased (dominated) for a short period of about 18:20–18:30 UT, which would be expected to reduce the reconnection rate at the dayside magnetopause.

A large polar cap ionization patch formed in the cusp region near noon between about 18:30 and 19:30 UT, giving a local enhancement in TEC, and subsequently crossed through the throat into the polar cap along plasma flow streamlines [Zhang et al., 2013]. During the evolution of the patch within the polar cap, two DMSP satellite passes (by F16 and F17) intersected it. Figure 2 reveals the distributions of the O^+ number density and horizontal ion flow along the orbits of the DMSP F16 and F17 satellites at about 860 km,

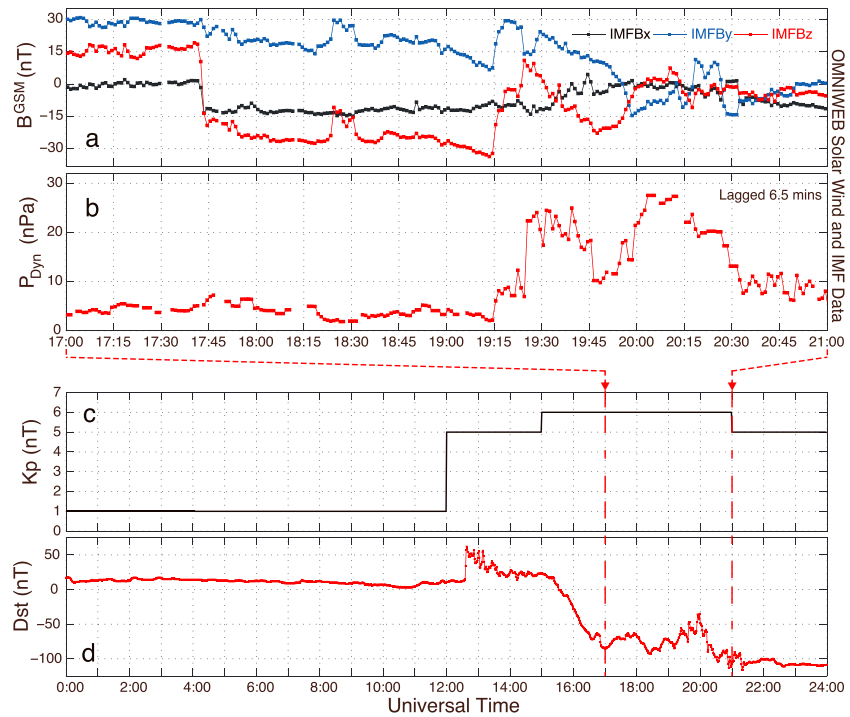


Figure 1. An overview of the solar wind and IMF conditions on 26 September 2011. Parameters shown are (a) the IMF components in GSM coordinates, (b) the solar wind dynamic pressure, P_{dyn} , (c) the Kp index, and (d) the Dst index (SYM-H). The IMF and solar wind data were shifted by about 6.5 min (suggested by Time History of Events and Macroscale Interactions during Substorms (THEMIS) A observations, shown in reference Zhang *et al.* [2013]) from the nose of Earth's bow shock to the subsolar magnetopause.

projected onto the maps of the TEC and flow streamlines. The location of the plasma patch is highlighted by the blue ellipse in each panel. The F16 satellite initially crossed the leading edge of the patch, after which F17 crossed through the front part of the patch, around the center of the polar cap region. The satellites observed well-defined enhancements in the O^+ number density when they encountered the patch (Figures 2 and 3a),

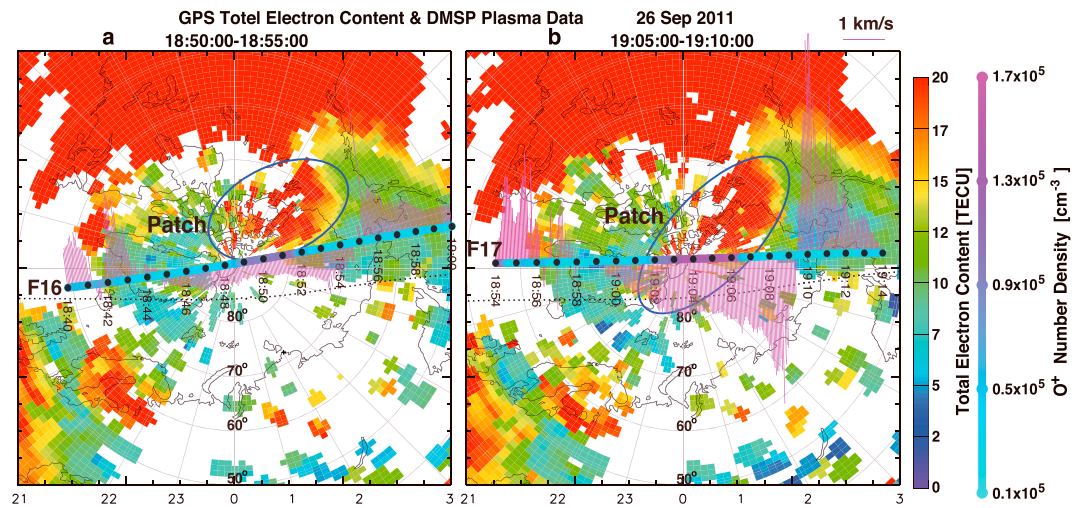


Figure 2. The in situ ion parameters measured by DMSP F16 and F17 projected onto the 2-D maps of median-filtered TEC on a geomagnetic latitude/magnetic local time (MLT) grid [Thomas *et al.*, 2013; Zhang *et al.*, 2013]. The projected orbits of F16 and F17 are shown by the colored thick line, where the color scale shows the O^+ number density. The mauve drift vectors (perpendicular to the orbit) show the measured horizontal ion flow. The dotted line across each panel is the day-night terminator at 100 km altitude.

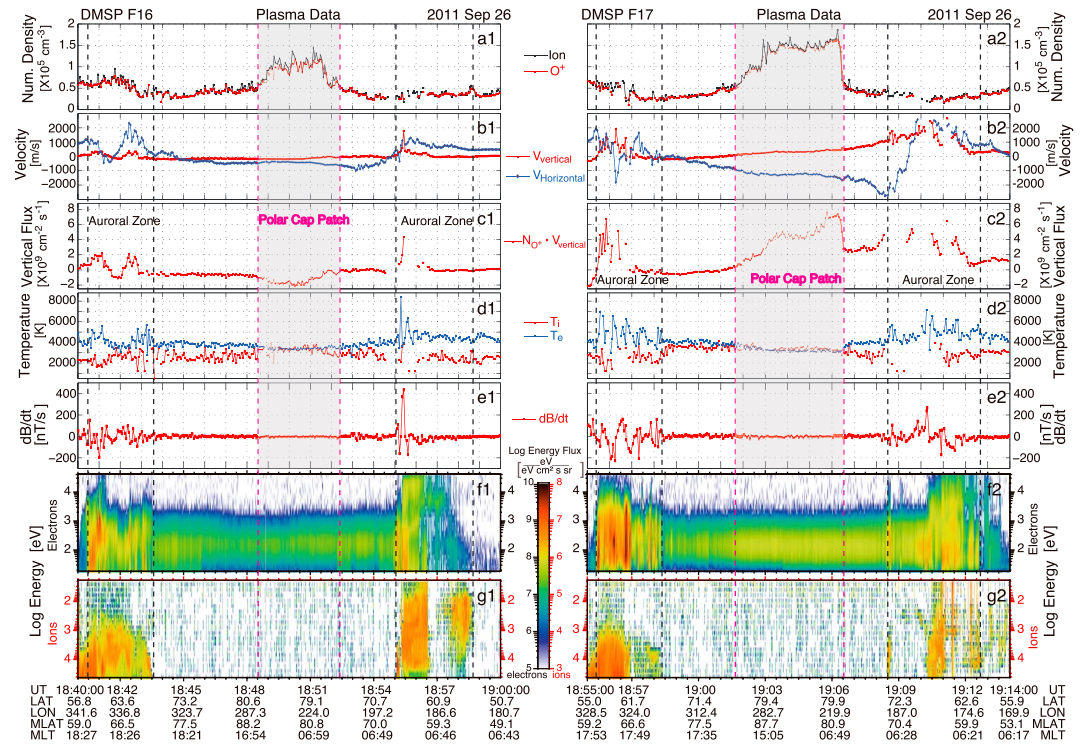


Figure 3. A time series of in situ plasma parameters measured by DMSP F16 and F17, respectively. Parameters shown are (a1 and a2) plasma number densities for O^+ and total ions, (b1 and b2) the cross-track vertical and horizontal ion flow, (c1 and c2) the vertical ion flux of thermal O^+ , (d1 and d2) the ion and electron temperature, (e1 and e2) the estimated field-aligned current by using dB/dt , (f1 and f2) the electron energy flux, and (g1 and g2) the ion energy flux. The vertical dashed lines separate the approximate locations of the auroral zone and polar cap patch (also highlighted by the grey area), respectively.

while the TEC within the patch remained fairly stable throughout the passes of the two DMSP satellites. In addition, the ion velocities measured by the satellites confirmed the observation of a two-cell convection pattern by the SuperDARN radars (Figures 4a–4c) and the prediction from the expanding-contracting polar cap model (ECPC) [Cowley and Lockwood, 1992]. The measured flows were enhanced by about a factor of 3 during the F17 pass (Figure 2b) compared to those in the F16 pass (Figure 2a), which would be expected to produce significant frictional heating of the ions [Loranc and St.-Maurce, 1994; Wilson, 1994]. Note that the patch did not extend across the whole east-west extent of the antisunward convection region in the polar cap.

Both satellites crossed the auroral zone before and after traversing the polar cap region. In the auroral zone, the plasma number density was not consistently enhanced in the topside ionosphere (about 860 km, Figure 3a), with only a weak enhancement seen in the dusk oval early in the passes. The vertical velocity in the auroral zone, however, was strongly upward and impulsive, a potential signature of wave heating process (Figure 3b), which can still result in strong upward ion flux (Figure 3c). We interpret these events as auroral bulk ion upflows, which are accompanied with an enhanced electron temperature (Figure 3d, $T_e > T_i$), notable field-aligned current sheets or filaments (Figure 3e) and enhanced electron and ion energy fluxes from the magnetosphere (Figures 3f and 3g). The ion upflows appear to be roughly correlated with the variations in the magnitudes of the field-aligned currents. The auroral bulk upflows are much larger in the observations from F17 than in those from F16.

After entering the polar cap region, both satellites measured stable conditions in all the parameters until they encountered the polar cap patch. The F16 satellite crossed only the leading edge of the patch (Figure 2a), where the ion number density, dominated by O^+ , increased by about a factor of 2; the vertical ion flows were steady and downward, resulting in downward enhancements of O^+ vertical flux; the ion temperature was elevated to a similar temperature to the electrons ($T_i \approx T_e$), the estimated field-aligned currents were near zero, and the electron energy fluxes were low, mainly confined to energies < 1 keV. These downward O^+ fluxes are

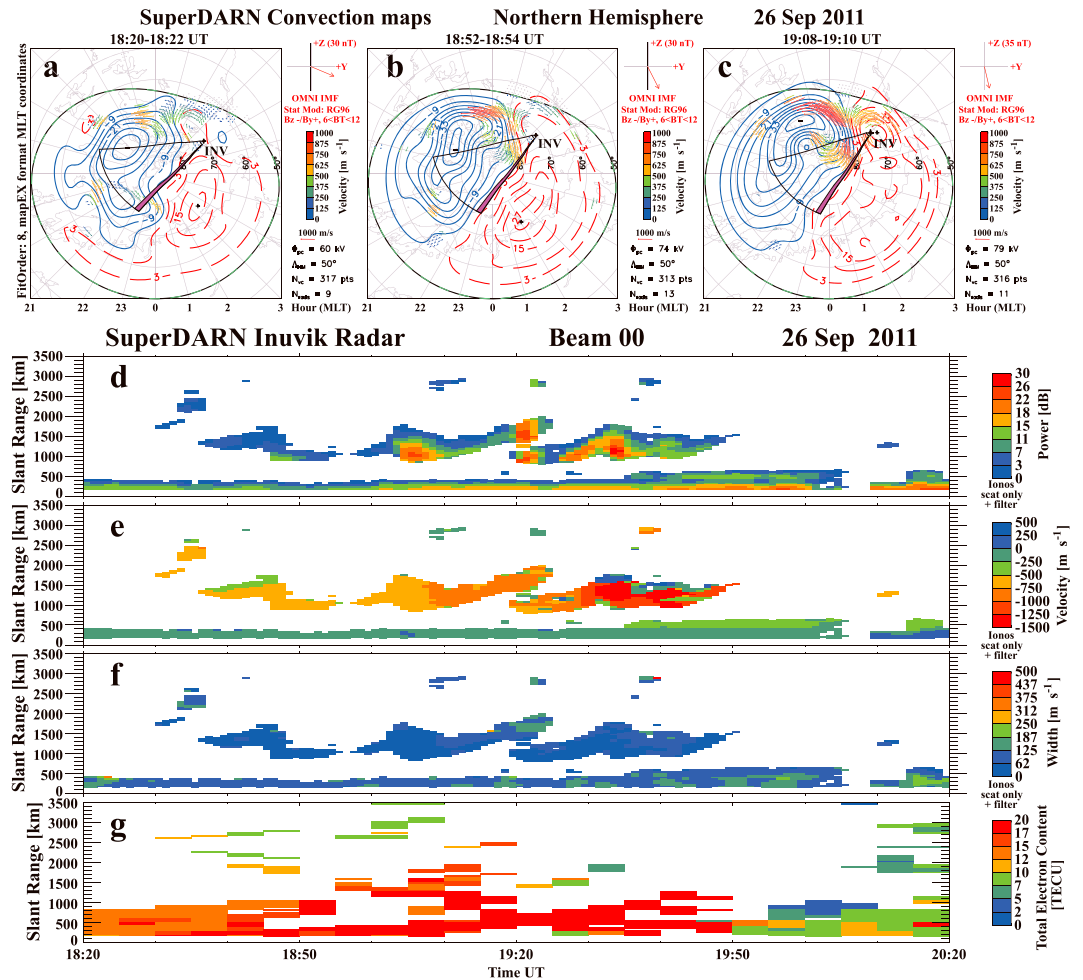


Figure 4. Extracts from a full series of 2-D maps of ionospheric convection pattern on a geomagnetic latitude/MLT grid with noon at the top, together with a time series of ionospheric backscatter, seen from the beam 0 of SuperDARN Inuvik radar and the GPS TEC along that beam. The field of view of SuperDARN Inuvik radar is presented as a fan with beam 0 highlighted as the purple area in each convection map. The direction and magnitude of the lagged IMF are indicated at the right-hand upper corner of each map.

interpreted to be heavy ions originally accelerated by the cusp/left ion fountain, returning due under the action of gravity [Lockwood *et al.*, 1985a, 1985b; Redmon *et al.*, 2010].

The satellite F17 crossed deeper into the front part of the patch about 12 min later (Figure 2b). At this time, the O^+ number density was enhanced by about a factor of 3 and the horizontal velocity of the plasma has increased from about 400 to 1200 m/s. The corresponding vertical ion flow speeds are increased and upward, and the resulting upward O^+ vertical flux was consequently strong (reaching about $7 \times 10^9 \text{ cm}^{-2} \text{ s}^{-1}$). The estimated field-aligned currents were again near zero, and there was strong soft electron precipitation over the whole polar cap pass (not only in the patch) with electron energies in the range $\sim 50\text{--}300 \text{ eV}$ (Figure 3f2).

3. Discussion

Figure 1a shows that there is a short period of decreasing IMF B_z and increasing B_y (which becomes the dominant component) from about 18:20 to 18:30 UT. This would be expected to reduce the reconnection rate at the dayside magnetopause, consistent with the weak flows (about 500 m/s) near the cusp “throat” (seen in Figure 4a). After the IMF returned strongly southward, there were flow bursts (up to about 1200 m/s) near the cusp region, associated with pulsed dayside reconnection (Figures 4b and 4c) [e.g., Wild *et al.*, 2001; Zhang *et al.*, 2011b]. Assuming that the distance between the poleward edge of the cusp region and the center

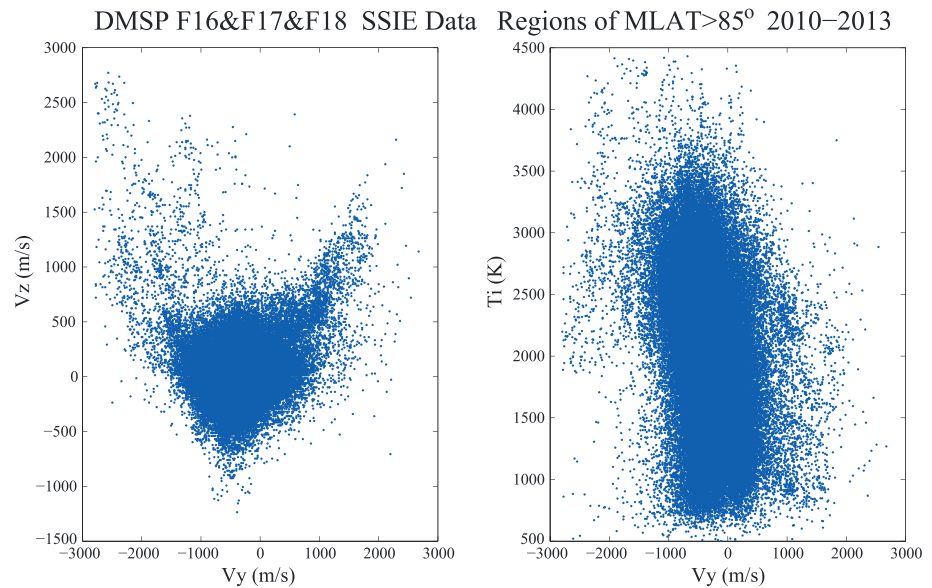


Figure 5. Scatterplots showing the relationship between (a) the vertical velocity, V_z , and the cross-track horizontal velocity, V_y , and (b) the ion temperature, T_i and V_y , for all of the crossings of the center polar cap region (magnetic latitude (MLAT) $> 85^\circ$) by DMSP F16–F18 from 2010 to 2013. The positive V_y represents sunward horizontal flow and negative represents antisunward flow, while the V_z positive is upward and negative is downward.

of the polar cap is about 1000 km, we can roughly estimate that the ionospheric plasma would need about 33 and 15 min to transit from the cusp region to the locations of the F16 and F17 passes, respectively, based on the flow enhancements observed by F16 and F17 and by SuperDARN radars (Figures 2, 4b, and 4c). The SuperDARN Inuvik radar covers the region of interest, with beam 0 pointing nearly along the convection streamlines. This beam recorded three clear poleward moving structures, starting at a distance about 800 km from the radar, during the periods 18:25–18:54, 18:56–19:24, and 19:18–19:50 UT approximately (Figures 4d–4f). These observations are consistent with the well-known propagating ionospheric signatures of pulsed reconnection at the dayside magnetopause [Wild *et al.*, 2001; Zhang *et al.*, 2008] and are associated with the poleward evolving patches (Figure 4g). This strongly suggests that the ionospheric flow bursts and the plasma patches are both generated by pulsed dayside reconnection, due to the strong southward IMF conditions.

In the polar cap, the plasma flux in the topside ionosphere is usually expected to be downward, due to the action of gravity on the heavy ions previously driven upward in the cusp/cleft ion fountain [Lockwood *et al.*, 1985a, 1985b; Redmon *et al.*, 2010]. However, the field-aligned flow can turn upward when rapid antisunward flows appear, with consequent significant frictional heating of the ions, which overcomes the gravity effect. This increase in the vertical ion flux is associated with an elevated density at higher ionospheric altitudes in the polar cap. As an example, the observations from F16 offer us a picture in which downward fluxes dominated the polar cap while the antisunward flows were too weak to produce enough frictional heating of the ions to drive upward flow (Figures 2a and 3a), whereas the vertical velocity, measured by F17, turned upward and increased in magnitude as the antisunward flows became enhanced to values above 800 m/s (Figures 2b and 3b). Although there was a strong correlation between the magnitude of the cross-track flow and the response of the vertical flow in the polar cap, the magnetic dip angle is very high and the contribution of the horizontal flow to the vertical flow is very small. An extensive survey has been performed for all of the crossings of the central polar cap region (magnetic latitude greater than 85°) by F16–F18 from 2010 to 2013 (Figure 5). The scatterplot includes the data from 16,025 DMSP transpolar orbits, in which 47.6% of points have positive V_z ($V_z > 0$) and 52.4% of points have negative V_z . The scatterplot in Figure 5 (left) shows a clear “V”-shape trend to the vertical velocity, V_z , that is upward and increased in magnitude when the cross-track horizontal velocity, V_y , becomes enhanced above a certain value, which may be dependent on the magnetic conditions at that time. It is certainly possible that large horizontal flows, such as implied in this study, give rise to non-Maxwellian velocity distributions for which a fit to a Maxwellian will yield an apparently high value. The horizontal and vertical drifts are derived by locating the centroid of a distribution for which the “thermal” width is small compared to the

vehicle speed of 7.5 km/s. Assuming this is the case, even a non-Maxwellian distribution will produce relatively small uncertainties in the derived vertical and horizontal drifts shown here. The scatterplot in Figure 5 (right) also shows a clear increasing trend in the ion temperature as V_y becomes enhanced, especially for negative values of V_y . Thus, the statistical results confirm that the field-aligned flow can turn upward when rapid antisunward flows appear, with consequent significant frictional heating of the ions, which overcomes the gravity effect.

Frictional heating of the ions maximizes near the F peak, and it is in this region where the plasma pressure is increased and thus produces upward flow. At higher altitudes in the topside ionosphere, we may observe upward flows of the ions but the ion temperature will not be highly elevated because the upward flow is associated with adiabatic cooling of the gas [Heelis *et al.*, 1993]. Thus, we would not normally expect to see evidence of Joule heating in the topside ionosphere at high latitudes. The F17 data showed that the polar cap ion temperature was indeed enhanced (Figure 3d2). Thus, we propose that the observed O^+ upflows were mainly accelerated by frictional heating due to rapid plasma flows in the polar cap. Although both energetic particle precipitation and frictional heating were taking place in the cusp region, the flow enhancement extended over a wider area and was thus able to drive upflows over a large region of the polar cap. The ion upflow flux, the prime parameter of interest in terms of the contribution to polar ion outflow, was thus a multiplication of the density enhancement (i.e., the patch) generated and transported from the dayside, and the ion upward velocity, presumably related to frictional heating produced by rapid antisunward flows. The upward ion flux was very strong at times, mainly due to the enhanced density contained in the patch. These large fluxes of upwelling ions, therefore, could form an abundant seed population that might be further heated at higher altitudes to escape velocity by various energization processes [Yau and Andre, 1997; Andre and Yau, 1997; Moore *et al.*, 1997; Strangeway *et al.*, 2005; Sharp *et al.*, 1977]. Note that there was a sharp density boundary when F17 exited the dawnside edge of the patch region. This occurred because the horizontal convective flows, measured by F17 and the SuperDARN radars, had a component normal to this boundary (pointing duskward), with weaker flows inside the patch (higher-density region) and stronger flows outside it (lower density region), although the SuperDARN 2-D convection pattern was dependent on the statistical convection model [Ruohoniemi and Baker, 1998] due to a lack of sufficient echoes in this region. The existence of this flow gradient therefore produced a “steepened” boundary. This gradient did not correspond to higher T_i , as would be expected if the lower densities were produced by enhanced loss rates associated with the faster flows. Thus, this gradient appeared to be caused by the spatial distribution of the source plasma that was subsequently convected to the satellite path.

Acknowledgments

This work in China was supported by the National Basic Research Program (grant 2012CB825603), the National Natural Science Foundation (grants 41574138, 41274149, and 41274148), the Shandong Provincial Natural Science Foundation (grant JQ201412), and the International Collaboration Supporting Project, Chinese Arctic and Antarctic Administration (IC201511). The work at Reading University was supported by STFC consolidated grant ST/M000885/1. The Norwegian contribution was supported by the Research Council of Norway grant 230996. We are grateful to C.Y. Tu for his helpful discussions. SuperDARN is a collection of radars funded by national scientific funding agencies in Australia, Canada, China, France, Japan, South Africa, United Kingdom, and United States of America. The Virginia Tech authors acknowledge the support of NSF awards AGS-0946900 and AGS-0838219 and a graduate research fellowship from the Virginia Space Grant Consortium. The work at the University of Leicester is supported by NERC grant NE/K011766/1. The GPS TEC acquisition effort is led by A.J. Coster at MIT Haystack Observatory. The GPS TEC and SuperDARN data are available on the public database: <http://vt.superdarn.org/tiki-index.php?page=DaViT+TEC>. We also thank the NOAA FTP and JHU/APL for making available the DMSP data (ftp://ftp.ngdc.noaa.gov/STP/satellite_data/) and the NASA OMNIWeb for the solar wind, IMF (http://omniweb.gsfc.nasa.gov/html/sc_merge_data1.html).

4. Conclusions

The observations presented here provide an excellent record of two types of O^+ upwelling affecting the topside of the polar ionosphere: type one occurs within an ionization patch at the center of the polar cap region, associated with the frictional heating produced by rapid antisunward flows, and type two occurs within the auroral zone, associated with field-aligned currents. The polar cap patches provide an important source of upwelling ions which could form a seed population for plasma escape at higher altitudes. However, how the O^+ is further accelerated to produce outflow, and the resulting O^+ trajectories, are not yet well known. These are important subjects that will be addressed by the ongoing Enhanced Polar Outflow Probe (e-POP) mission [Yau and James, 2011] and by the future Magnetosphere-Ionosphere-Thermosphere Coupling Constellation mission [Liu *et al.*, 2014].

References

- Andre, M., and A. W. Yau (1997), Theories and observations of ion energization and outflow in the high latitude magnetosphere, *Space Sci. Rev.*, 80(1–2), 27–48.
- Axford, W. I. (1968), The polar wind and the terrestrial helium budget, *J. Geophys. Res.*, 73(21), 6855–6859.
- Carlson, H. C. (2012), Sharpening our thinking about polar cap ionospheric patch morphology, research, and mitigation techniques, *Radio Sci.*, 47, RS0L21, doi:10.1029/2011RS004946.
- Chappell, C. R., B. L. Giles, T. E. Moore, D. C. Delcourt, P. D. Craven, and M. O. Chandler (2000), The adequacy of the ionospheric source in supplying magnetospheric plasma, *J. Atmos. Sol. Terr. Phys.*, 62, 421–436.
- Chisham, G., *et al.* (2007), A decade of the Super Dual Auroral Radar Network (SuperDARN): Scientific achievements, new techniques and future directions, *Surv. Geophys.*, 28, 33–109.
- Coster, A. J., J. C. Foster, and P. J. Erickson (2003), Monitoring the ionosphere with GPS, *GPS World*, 14(5), 42–45.
- Cowley, S. W. H., and M. Lockwood (1992), Excitation and decay of solar-wind driven flows in the magnetosphere-ionosphere system, *Ann. Geophys.*, 10, 103–115.

- Crowley, G. (1996), Critical review of ionospheric patches and blobs, in *Review of Radio Science 1992–1996*, edited by W. R. Stone, pp. 619–648, Oxford Univ. Press, Oxford, U. K.
- Daglis, I. A. (1997), The role of magnetosphere-ionosphere coupling in magnetic storm dynamics, in *Magnetic Storms, Geophys. Monogr.*, vol. 98, edited by B. T. Tsurutani et al., pp. 107–116, AGU, Washington, D. C.
- Demars, H. G., and R. W. Schunk (2006), Seasonal and solar-cycle variations of propagating polar wind jets, *J. Atmos. Sol. Terr. Phys.*, *68*, 1791–1806.
- Dungey, J. W. (1961), Interplanetary magnetic field and the auroral zones, *Phys. Rev. Lett.*, *6*, 47–48.
- Foster, J. C., et al. (2005), Multiradar observations of the polar tongue of ionization, *J. Geophys. Res.*, *110*, A09S31, doi:10.1029/2004JA010928.
- Gardner, L. C., and R. W. Schunk (2007), Propagating plasma patch and associated neutral stream flows, *J. Atmos. Sol. Terr. Phys.*, *69*, 1884–1892.
- Greenwald, R. A., et al. (1995), DARN/SuperDARN: A global view of the dynamics of high-latitude convection, *Space Sci. Rev.*, *71*(1–4), 761–796.
- Hardy, D. A., et al. (1984), Precipitating electron and ion detectors (SSJ/4) for the block 5D/flights 6–10 DMSP (Defense Meteorological Satellite Program) satellites: Calibration and data presentation, Rep. AFGL-TR-84-0317, (Air Force Geophys. Lab., Hanscom Air Force Base, Mass).
- Heelis, R. A., G. J. Bailey, R. Sellek, R. J. Moffett, and B. Jenkins (1993), Field-aligned drifts in subauroral ion drift events, *J. Geophys. Res.*, *98*(A12), 21,493–21,499.
- Ho, C. W., J. L. Horwitz, N. Singh, and G. R. Wilson (1994), Effects of magnetospheric electrons on polar plasma outflow: A semikinetic model, *J. Geophys. Res.*, *97*(A6), 8425–8437.
- Hosokawa, K., T. Kashimoto, S. Suzuki, K. Shiokawa, Y. Otsuka, and T. Ogawa (2009), Motion of polar cap patches: A statistical study with all-sky airglow imager at Resolute Bay, Canada, *J. Geophys. Res.*, *114*, A04318, doi:10.1029/2008JA014020.
- Liu, Y., C. Wang, J. Y. Xu, and X. Y. Li (2014), Orbit requirements for detecting the upflow ion source region (in Chinese), *Chin. J. Space Sci.*, *34*(1), 104–108.
- Lockwood, M., and H. C. Carlson (1992), Production of polar cap electron density patches by transient magnetopause reconnection, *Geophys. Res. Lett.*, *19*, 1731–1734.
- Lockwood, M., and J. E. Titheridge (1981), Ionospheric origin of magnetospheric O⁺ ions, *Geophys. Res. Lett.*, *8*, 381–384.
- Lockwood, M., J. H. Waite Jr., T. E. Moore, J. F. E. Johnson, and C. R. Chappell (1985a), A new source of suprathermal O⁺ ions near the dayside polar cap boundary, *J. Geophys. Res.*, *90*, 4099–4116.
- Lockwood, M., M. O. Chandler, J. L. Horwitz, J. H. Waite Jr., T. E. Moore, and C. R. Chappell (1985b), The cleft ion fountain, *J. Geophys. Res.*, *90*, 9736–9748.
- Loranc, M., and J.-P. St-Maurice (1994), A time-dependent gyro-kinetic model of thermal ion upflows in the high-latitude F region, *J. Geophys. Res.*, *99*(A9), 17,429–17,451.
- Moore, T. E., et al. (1997), High-altitude observations of the polar wind, *Science*, *277*, 349–351.
- Oksavik, K., V. L. Barth, J. Moen, and M. Lester (2010), On the entry and transit of high-density plasma across the polar cap, *J. Geophys. Res.*, *115*, A12308, doi:10.1029/2010JA015817.
- Redmon, R. J., W. K. Peterson, L. Andersson, E. A. Kihn, W. F. Denig, M. Hairston, and R. Coley (2010), Vertical thermal O⁺ flows at 850 km in dynamic auroral boundary coordinates, *J. Geophys. Res.*, *115*, A00J08, doi:10.1029/2010JA015589.
- Rodger, A. S., M. Pinnock, J. R. Dudeney, K. B. Baker, and R. A. Greenwald (1994), A new mechanism for polar patch formation, *J. Geophys. Res.*, *99*(A4), 6425–6436.
- Ruohoniemi, J., and K. Baker (1998), Large-scale imaging of high-latitude convection with SuperDARN HF radar observations, *J. Geophys. Res.*, *103*(A9), 20,797–20,811.
- Schunk, R. W. (2007), Time-dependent simulations of the global polar wind, *J. Atmos. Sol. Terr. Phys.*, *69*, 2028–2047.
- Schunk, R. W., and J. J. Sojka (1989), A three-dimensional time-dependent model of the polar wind, *J. Geophys. Res.*, *94*, 8973–8991.
- Schunk, R. W., H. G. Demars, and J. J. Sojka (2005), Propagating polar wind jets, *J. Atmos. Sol. Terr. Phys.*, *67*(4), 357–364.
- Seki, K., R. C. Elphic, M. Hirahara, T. Terasawa, and T. Mukai (2001), On atmospheric loss of oxygen ions from Earth through magnetospheric processes, *Science*, *291*, 1939–1941.
- Semeter, J., C. J. Heinselman, J. P. Thayer, R. A. Doe, and H. U. Frey (2003), Ion upflow enhanced by drifting F-region plasma structure along the nightside polar cap boundary, *Geophys. Res. Lett.*, *30*(22), 2139, doi:10.1029/2003GL017747.
- Sharp, R. D., R. G. Johnson, and E. G. Shelley (1977), Observations of an ionospheric acceleration mechanism producing energetic (keV) ions primarily normal to the geomagnetic field direction, *J. Geophys. Res.*, *82*, 3324–3328.
- Shelley, E. G., R. G. Johnson, and R. D. Sharp (1972), Satellite observations of energetic heavy ions during a geomagnetic storm, *J. Geophys. Res.*, *77*, 6104–6110.
- Skjæveland, Å., J. Moen, and H. C. Carlson (2011), On the relationship between flux transfer events, temperature enhancements and ion upflow events in the cusp ionosphere, *J. Geophys. Res.*, *116*, A10305, doi:10.1029/2011JA016480.
- Skjæveland, Å., J. I. Moen, and H. C. Carlson (2014), Which cusp upflow events can possibly turn into outflows?, *J. Geophys. Res. Space Physics*, *119*, 6876–6890, doi:10.1002/2013JA019495.
- Stevenson, B. A., J. L. Horwitz, G. Germany, T. E. Moore, B. L. Giles, P. D. Craven, M. O. Chandler, Y.-J. Su, and G. K. Parks (2001), Polar observations of topside field-aligned O⁺ flows and auroral forms, *J. Geophys. Res.*, *106*(A9), 18,969–18,979, doi:10.1029/2000JA003042.
- Strangeway, R. J., R. E. Ergun, Y. J. Su, C. W. Carlson, and R. C. Elphic (2005), Factors controlling ionospheric outflows as observed at intermediate altitudes, *J. Geophys. Res.*, *110*, A03221, doi:10.1029/2004JA010829.
- Thomas, E. G., J. B. H. Baker, J. M. Ruohoniemi, L. B. N. Clausen, A. J. Coster, J. C. Foster, and P. J. Erickson (2013), Direct observations of the role of convection electric field in the formation of a polar tongue of ionization from storm enhanced density, *J. Geophys. Res. Space Physics*, *118*, 1180–1189, doi:10.1002/jgra.50116.
- Valladares, C. E., D. Alcaydé, J. V. Rodriguez, J. M. Ruohoniemi, and A. P. Van Eyken (1999), Observations of plasma density structures in association with the passage of traveling convection vortices and the occurrence of large plasma jets, *Ann. Geophys.*, *17*(8), 1020–1039.
- Wild, J. A., et al. (2001), First simultaneous observations of flux transfer events at the high-latitude magnetopause by the Cluster spacecraft and pulsed radar signatures in the conjugate ionosphere by the CUTLASS and EISCAT radars, *Ann. Geophys.*, *19*, 1491–1508.
- Wilson, G. R. (1994), Kinetic modeling of O⁺ upflows resulting from E × B convection heating in the high-latitude F region ionosphere, *J. Geophys. Res.*, *99*(A9), 17,453–17,466.
- Winglee, R. M. (2004), Ion cyclotron and heavy ion effects on reconnection in a global magnetosphere, *J. Geophys. Res.*, *109*, A09206, doi:10.1029/2004JA010385.
- Yau, A. W., and M. Andre (1997), Sources of ion outflow in the high latitude ionosphere, *Space Sci. Rev.*, *80*(1–2), 1–26.
- Yau, A. W., and H. G. M. P. James (2011), Scientific objectives of the Canadian CASSIOPE Enhanced Polar Outflow Probe (e-POP) small satellite mission, in *The Sun, the Solar Wind, and the Heliosphere, IAGA Special Sopron Book Series*, vol. 4, edited by M. P. Miralles and J. S. Almeida, pp. 355–364, Springer, Dordrecht, Netherlands.

- Yau, A. W., W. K. Peterson, and T. Abe (2011), Influences of the ionosphere, thermosphere and magnetosphere on ion outflows, in *The Dynamic Magnetosphere, IAGA Special Sopron Book Series*, vol. 3, edited by W. Liu and M. Fujimoto, pp. 283–314, Springer, Dordrecht, Netherlands.
- Zhang, Q. H., R. Y. Liu, M. W. Dunlop, J. Y. Huang, H. Q. Hu, M. Lester, Y. H. Liu, Z. J. Hu, Q. Q. Shi, and M. G. T. Taylor (2008), Simultaneous tracking of reconnected flux tubes: Cluster and conjugate SuperDARN observations on 1 April 2004, *Ann. Geophys.*, *26*, 1545–1557.
- Zhang, Q. H., et al. (2011a), On the importance of interplanetary magnetic field $|B_y|$ on polar cap patch formation, *J. Geophys. Res.*, *116*, A05308, doi:10.1029/2010JA016287.
- Zhang, Q. H., et al. (2011b), Coordinated Cluster/Double Star and ground-based observations of dayside reconnection signatures on 11 February 2004, *Ann. Geophys.*, *29*(10), 1827–1847.
- Zhang, Q. H., et al. (2013), Direct observations of the evolution of polar cap ionization patches, *Science*, *339*, 1597–1600.
- Zhang, Q.-H., M. Lockwood, J. C. Foster, S.-R. Zhang, B.-C. Zhang, I. W. McCrea, J. Moen, M. Lester, and J. M. Ruohoniemi (2015), Direct observations of the full Dungey convection cycle in the polar ionosphere for southward interplanetary magnetic field conditions, *J. Geophys. Res. Space Physics*, *120*, 4519–4530, doi:10.1002/2015JA021172.